Model for the Increase in Thruster Efficiency from Cross-Channel Coupling in Nested Hall Thrusters

IEPC-2019-204

Presented at the 36th International Electric Propulsion Conference
University of Vienna, Austria
September 15–20, 2019

Leanne L. Su,*
University of Michigan, Ann Arbor, MI 48109

Scott J. Hall,†
Vantage Partners, LLC, NASA Glenn Research Center, Cleveland, OH, 44135

Sarah E. Cusson,‡ and Benjamin A. Jorns§
University of Michigan, Ann Arbor, MI 48109

Multi-channel operation in nested Hall thrusters has been experimentally shown to enhance thruster efficiency compared to single-channel operation at constant power. This is the result of higher local neutral density due to the flow from adjacent channels, leading to two effects: neutral ingestion and decreased plume divergence. Analytical expressions for the impact of these cross-channel effects on efficiency are derived for a nested Hall thruster based on the flow of neutrals between channels. These expressions are dependent on the geometry and operation of a given thruster, as well as its performance in single-channel operation. The mass utilization efficiency increase from cross-channel neutrals is found to be primarily driven by the distance between adjacent channels. A comparison of the model predictions of efficiency to experiment also shows agreement within uncertainty. These results are discussed in the context of best practices for nested Hall thruster channel testing and optimal thruster design.

*Ph.D Pre-Candidate, Department of Aerospace Engineering, leannesu@umich.edu
†Research Engineer, Electric Propulsion Systems Branch, scott.j.hall@nasa.gov
‡Ph.D. Candidate, Department of Aerospace Engineering, cusson@umich.edu
§Assistant Professor, Department of Aerospace Engineering

Nomenclature

A_{NHT} = cross-channel neutrals surface area
A_{ch} = discharge channel surface area
A_{exp} = expansion front surface area
I_b = ion beam current
I_d = discharge current
P_d = discharge power
T = thrust
V_a = acceleration voltage
V_d = discharge voltage
V_l = ion loss voltage
Z_i = charge state of the i^{th} ion species
Ω_i = current fraction of the i^{th} ion species
$\dot{m}_a$ = anode mass flow rate
$\dot{m}_b$ = ion beam mass flow rate
$\dot{m}_{NHT}$ = cross-channel mass flow rate
$\dot{m}_{ch}$ = channel mass flow rate
$\dot{m}_{fac}$ = facility neutral mass flow rate
η_a = anode efficiency
η_b = current utilization efficiency
η_d = plume divergence utilization efficiency
η_m = mass utilization efficiency
η_q = charge utilization efficiency
η_v = voltage utilization efficiency
η_{NHT} = efficiency increase from cross-channel effects
$\eta_{d,NHT}$ = efficiency increase from divergence angle reduction
η_{fac} = facility mass flow rate
$\eta_{m,NHT}$ = efficiency increase from neutral ingestion
γ_{ij} = geometry factor
θ = plume divergence angle
ε = electron current fraction, $\frac{I_e}{I_d}$
φ = angle to ionization plane
ξ = exchange ratio, $\frac{m_{Xe} I_d}{\dot{m}_a e}$
ζ = ionization plane scaling factor
a = torus major axis
b = torus minor axis
m_{Xe} = mass of a Xenon ion
n_n = neutral density
r = radial position
v_{th} = thermal speed
z_{NHT} = height of ionization plane

I. Introduction

High-power electric propulsion (EP) is considered an enabling technology for many deep space missions as it offers significant mass and cost savings when compared to traditional chemical propulsion systems. EP missions are often associated with longer trip times, but the increased deliverable payload still makes these architectures an attractive option. Additionally, for cargo missions, there is minimal downside to an increase in trip time. Indeed, studies show that separating crewed deep space travel into crew and cargo missions leads to significant reductions in launch costs and travel times for the crew.[1] For these missions to be possible, 50 to 100-kW class EP systems must be developed to enable such cargo transports.[2] A 300 to 700-kW system with multiple 100-kW thrusters could facilitate missions to near-Earth asteroids, Mars moons, and the Martian surface.[1–4] The development of a high-power EP system is vital for constructing the necessary infrastructure for crewed missions in deep space.

While there are a number of EP systems that are scalable to these power levels, Hall thrusters are a competitive option due to their extensive heritage and high Technology Readiness Level. They have been used on satellites for station-keeping and orbit-raising for decades.[5] Recently, there has been substantial research to broaden the capability of Hall thrusters to include interplanetary cargo missions as well as other mission spaces.[2] However, challenges associated with large footprints and masses present themselves at the higher powers necessary for these missions. Nested Hall thrusters (NHTs) offer a potential solution to these challenges. The NHT architecture concentrically nests multiple discharge channels around a single centrally-mounted cathode, allowing thrusters to scale to high power with much smaller footprints than their single-channel counterparts of equal power levels.[6] This enables NHTs to reach operational powers of 100 kW and beyond with reduced thruster specific masses.[7] Another advantage inherent to the design of NHTs is their capability for efficient performance over a more expansive throttling range than single-channel thrusters due to the ability to selective turn on or off channels.

These apparent advantages and the feasibility of NHTs have been explored most recently through an ongoing, decade-long effort based partially at the University of Michigan (UM).[8] The first prototype created through this program was the X2, a two-channel 10-kW class thruster developed by UM in conjunction with the Air Force Research Laboratory.[8] This proof-of-concept thruster demonstrated the viability of nested operation and offered a wider throttling envelope. After the validation of the nested concept, work began on the X3, a three-channel 100-kW class NHT. The X3 was developed at UM in partnership with the Air Force Research Laboratory, NASA Glenn Research Center, NASA Jet Propulsion Laboratory, and ElectroDynamic Applications.[9] UM began work on the X3 in 2009 and first fired it in 2013.[10] In 2015, the X3 was selected as part of NASA's NextSTEP project, a three-year program to further mature high-power electric propulsion systems for long duration deep-space missions. Under the NextSTEP program, the X3 demonstrated operational success with efficiencies over 60%, power levels up to 102 kW, and thrust up to 5.4 N.[11] Additionally, the X3 demonstrated thermal steady-state operation at 72 kW.[12]

While the X3, the most recent iteration of nesting technology, has exhibited promising performance comparable to current state-of-the-art Hall thrusters, there still remain fundamental open questions about the operation of NHTs. Examples include extending NHT lifetimes using magnetic shielding and the impact of multiple plasma discharges in close proximity on the operation of these devices.[13] One particularly intriguing area of ongoing investigation is the role of cross-channel coupling effects on thruster performance. Previous studies on both the X2 and X3 have indicated that multi-channel operation enhances both thrust and efficiency by improving the mass utilization efficiency and the beam divergence efficiency.[14] These two effects are believed to be the result of ingestion of un-ionized

neutral gas from adjacent channels.[14–17] For example, Cusson et al.'s work on the X2 showed that NHT efficiency improvements are due to thrust augmentation from neutral ingestion and plume divergence angle reduction, caused by neutral flow from adjacent channels.[14] Hall's work similarly provided evidence that the ingestion of un-ionized neutrals on the X3 can enhance performance.[15]

While there now appears to be a correlational explanation for the performance enhancement of nested Hall thrusters due to cross-channel effects, there has yet to be a predictive model for these effects. Such a tool would would be useful both for design and testing. For example, if we could determine how the geometry and operational conditions of a given thruster affect the magnitude of these cross-channel phenomena, we may be able to identify optimal design strategies. An equally important capability is being able to predict the role of cross-channel effects in enhancing single channel performance, as this could significantly reduce the testing burden for NHTs. Indeed, the power and throughput requirements of NHTs such as the X3 make full-scale testing difficult and expensive. If individual channels could be characterized and a model used to extrapolate to full channel prediction, this would substantially reduce facility usage. With these advantages in mind, there is an apparent need for a model to predict the impact of cross-channel interactions on NHT efficiency based on thruster geometry and single-channel performance.

In order to accomplish these goals, our paper is organized as follows: first, we discuss the existing framework for single-channel Hall thruster efficiency. Secondly, we introduce proposed modifications to this framework to account for neutral ingestion and plume divergence effects from cross-channel effects in an NHT. Next, we formulate a geometric argument for neutral ingestion from adjoining channels and develop semi-empirical expressions for how this ingestion impacts mass utilization and plume divergence. Finally, we compare the results from our model to experimental data from the X2 and X3 and discuss the implications of our results for both design and NHT testing.

II. Theory

In this section, we outline the efficiency model for cross-channel effects on an NHT. First, we review the existing framework for a single-channel Hall thruster phenomenological efficiency model. Then, we use a few key assumptions that allow us to develop modifications for a multi-channel efficiency model for NHTs that takes into account both the effect of neutral ingestion on the mass utilization efficiency and the effect of higher local neutral density on the plume divergence efficiency.

A. Single-channel Phenomenological Efficiency Model

Previous work has shown that near-field neutral density appears to drive cross-channel coupling effects,[14,15] so we aim to identify how the efficiency enhancements seen for multi-channel operation depend on this parameter and to determine scaling laws. To this end, we begin with a review of the single-channel Hall thruster phenomenological efficiency model[18–21] before expanding it to include effects from multiple channels.

For a single channel thruster, following Refs. 18 and 19, the anode efficiency is defined as

$$\eta_a = \frac{T^2}{2\dot{m}_a P_d} = \eta_q \eta_v \eta_b \eta_m \eta_d, \tag{1}$$

where T is thrust, $\dot{m}_a$ is prescribed mass flow through the anode, and P_d is power. The five partial efficiencies that the anode efficiency is decoupled into processes by which the thruster can experience losses in efficiencies and are outlined as follows.

1) *Charge utilization efficiency*: The decrease in efficiency from multiply-charged ions in the beam is defined as

$$\eta_q = \frac{\left(\sum \frac{\Omega_i}{\sqrt{Z_i}}\right)^2}{\sum \frac{\Omega_i}{Z_i}}, \tag{2}$$

where Ω_i is the current fraction of the i^{th} ion species, $\frac{I_i}{I_d}$, and Z_i is the charge state of the i^{th} ion species.

2) *Voltage utilization efficiency*: The conversion of voltage into ion velocity is defined as

$$\eta_v = \frac{V_a}{V_d} = 1 - \frac{V_l}{V_d}, \tag{3}$$

where V_d is the discharge voltage, V_a is the average acceleration voltage, and V_l is the ion loss voltage, $V_a - V_d$.

3) *Current utilization efficiency*: The fraction of ion current contained in the discharge current is defined as

$$\eta_b = \frac{I_b}{I_d} = 1 - \varepsilon, \tag{4}$$

where I_d is the discharge current, I_b is the ion beam current $\sum_i I_i$, where I_i is the current contribution from the i^{th} current species, and ε is the electron current fraction, $\frac{I_e}{I_d}$.

4) *Mass utilization efficiency*: The conversion of neutral mass flux into ion mass flux is defined as

$$\eta_m = \frac{\dot{m}_b}{\dot{m}_a} = \frac{\frac{m_{Xe} I_b}{e} \sum_i \frac{\Omega_i}{Z_i}}{\dot{m}_a} = \xi \eta_b \sum \frac{\Omega_i}{Z_i}, \tag{5}$$

where $\dot{m}_a$ is anode mass flow rate, $\dot{m}_b$ is the ion beam mass flow rate, and ξ is a value defined as the exchange ratio.

5) *Plume divergence efficiency*: The decrease in axially-directed momentum from divergence of the ion beams is defined as

$$\eta_d = (\cos\theta)^2, \tag{6}$$

where θ is the angle of plume divergence from channel centerline.

B. Multi-channel Phenomenological Efficiency Model

For a nested Hall thruster like the one seen in Fig. 1b, the thrust and efficiencies from all channels must be accounted for in the calculation of both the anode efficiency and the partial efficiencies defined in the previous section. To this end, we make a few key assumptions in the following derivation: first, that there are no multiply-charged ions such that $\eta_q = 1$; second, that the current utilization efficiency η_b is identical for all channels on a given thruster; and third, that the acceleration voltage V_a and therefore voltage utilization efficiency η_v are identical for all channels on a given thruster. Previous studies have shown that for a specific thruster at a given voltage and current density, the current and voltage utilization efficiencies remain relatively constant (within 1%).[18,22] Although our assumption of singly-charged ions may be flawed,[15] we use it to simplify our analysis and focus in on NHT effects only for this first-pass analysis.

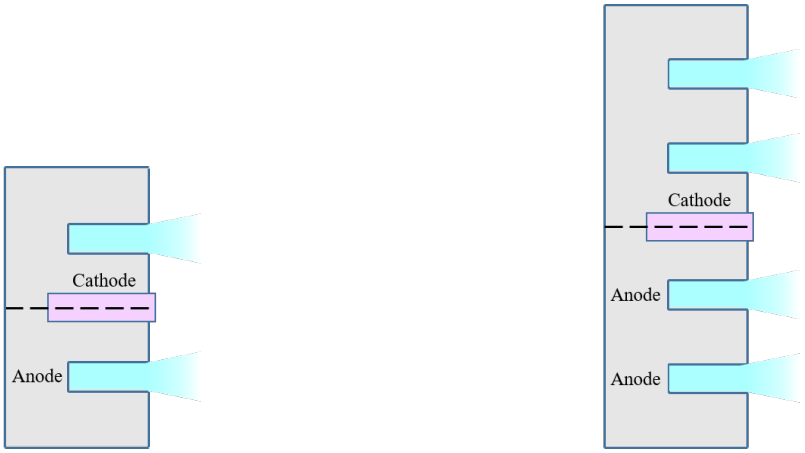

(a) Single-channel Hall thruster **(b) Nested-channel Hall thruster**

Fig. 1 Cross-sectional view of Hall thrusters with cylindrical axis of symmetry denoted by the dashed line.

Neglecting charge utilization efficiency, we can redefine the rest of the partial efficiencies seen in Eq. 1. For simplicity, the same subscripts are used for multi-channel efficiency as for single-channel efficiency except where necessary. The voltage utilization efficiency (Eq. 3) and current utilization efficiency (Eq. 4) remain the same, with the added definition that both the beam and discharge currents are now equal to the sum of currents to each channel. This modification can be seen in Eq. 7:

$$\begin{aligned} I_d &= \sum_i I_{d,i} \\ I_b &= \sum_i I_{b,i}, \end{aligned} \tag{7}$$

where i now describes each channel.

1. Mass Utilization Efficiency Modification

Previous studies have investigated the contribution from finite facility background pressures to the thrust and efficiency of Hall thrusters,[23–27] as well as how to model this contribution for a given facility

and thruster.[28] Frieman et al.'s model allows us to solve for the mass flow rate into the channel from facility effects, $\dot{m}_{fac}$. Before redefining the mass utilization efficiency for NHTs, it is useful to define $\dot{m}_{ch,i}$ as the total neutral mass flow into a given channel; this includes $\dot{m}_{fac,i}$, neutrals from high facility background pressure, and $\dot{m}_{NHT,i}$, the un-ionized propellant from adjacent channels:

$$\dot{m}_{ch,i} = \dot{m}_{a,i} + \dot{m}_{fac,i} + \dot{m}_{NHT,i}. \tag{8}$$

Note that the total neutral mass flow into a given channel is simply the sum of all channel neutral inflow terms and the total ion beam current is the sum of all:

$$\dot{m}_{ch} = \sum_i \dot{m}_{ch,i}. \tag{9}$$

We can now separate out our traditional mass utilization efficiency from Eq. 5 into a term η_{m0} that defines the thruster's ability to convert all the input neutral flow to output ion flow, a term $\eta_{m,fac}$ that isolates extra neutrals from facility background pressures, and a term $\eta_{m,NHT}$ that defines the boost the thruster receives from cross-channel neutrals alone:

$$\eta_m = \frac{\dot{m}_b}{\dot{m}_{ch}} \frac{\dot{m}_{ch}}{\dot{m}_a} = \frac{\dot{m}_b}{\dot{m}_{ch}} \frac{\sum_i \left(\dot{m}_{a,i} + \dot{m}_{fac,i}\right)}{\dot{m}_a} \frac{\dot{m}_{ch}}{\sum_i \left(\dot{m}_{a,i} + \dot{m}_{fac,i}\right)} = \eta_{m0} \cdot \eta_{m,fac} \cdot \eta_{m,NHT}, \tag{10}$$

where the new efficiencies are defined as

$$\eta_{m0} = \frac{\dot{m}_b}{\dot{m}_{ch}}, \tag{11}$$

$$\eta_{m,fac} = \frac{\sum_i \left(\dot{m}_{a,i} + \dot{m}_{fac,i}\right)}{\dot{m}_a}, \tag{12}$$

and

$$\eta_{m,NHT} = \frac{\dot{m}_{ch}}{\sum_i \left(\dot{m}_{a,i} + \dot{m}_{fac,i}\right)}. \tag{13}$$

Assuming that a given thruster's overall capability of converting neutral mass flow to ion mass flow does not vary from single-channel to multi-channel operation, η_{m0} for multi-channel operation should be identical to the η_m defined for single-channel operation. While η_{fac} would still be present in calculating single-channel Hall thruster efficiencies due to the presence of facility pressure effects, $\eta_{m,NHT}$ exists uniquely for NHTs due to cross-channel neutral ingestion. Additionally, this efficiency boost would still be seen for on-orbit operation, whereas the increase from facility background pressure would be lost.

While a general model based on geometry exists for determining $\dot{m}_{fac}$, no such model exists for $\dot{m}_{NHT}$. We derive such a model for cross-channel neutral mass flow rate to a given channel i, dependent on the anode mass flow into the adjacent channels j and a geometry factor γ_{ij} between channels:

$$\dot{m}_{NHT,i} = \sum_j \dot{m}_{a,j} \gamma_{ij}. \tag{14}$$

In this expression, γ_{ij} represents the geometry factor between channels, a term that describes how easily neutral gas can cross over between a given set of channels, and $\dot{m}_{a,j}$ represents the prescribed anode flow to each neighboring channel j. While Hall evaluated this correction empirically,[15] one of the major contributions is this work is to formulate an expression for γ_{ij} as a function of the total surface area and mass utilization efficiency of the adjacent channel in single-channel operation, as well as the distance between channels. This derivation will be presented in Section III.

2. Plume Divergence Efficiency Modification

For the impact on divergence efficiency from cross-channel coupling, our approach is more empirical in nature. This is because while the role of neutral ingestion in enhancing thruster performance is well-understood, the impact of neutrals on the divergence angle has only been studied empirically.[26,29] However, it is known that the divergence angle decreases with facility pressure and therefore neutral density.[30–32] By assuming a dependence of θ on n_n, we can perform a first-order Taylor expansion to get the following relation for divergence angle for a given channel:

$$\theta_i = \theta_{0,i} + \frac{\partial \theta}{\partial n_n} \delta n_{n,i}, \tag{15}$$

where $\theta_{0,i}$ is the divergence angle for single-channel operation of a given channel, $\frac{\partial \theta}{\partial n_n}$ is the change in divergence angle due to a small change in neutral density, and δn_n is a small change in neutral density in front of a given channel. The relation for $\frac{\partial \theta}{\partial n_n}$ was found by compiling multiple sets of experimental data[30–32] and using the ideal gas law to calculate change in neutral density for a given change in facility pressure. This is related to the discharge voltage as follows:

$$\frac{\partial \theta}{\partial n_n} = (3.49 \times 10^{-21}) V_d - 5.82 \times 10^{-18}. \tag{16}$$

The linear fit shown in Eq. 16 is plotted against the data in Fig. 2.

The small change in neutral density is calculated from $\dot{m}_{NHT.i}$ as follows:

$$\delta n_{n,i} = \frac{(1 - \eta_{m,i}) \dot{m}_{NHT,i}}{m_{Xe} A_{ch,i} v_{th}}, \tag{17}$$

where $A_{ch,i}$ is the total exit plane surface area of a given discharge channel as seen in Fig. 3, v_{th} is the thermal speed based on anode temperature, $\sqrt{\frac{8 k_B T}{\pi m_{Xe}}}$, and $\eta_{m,i}$ is the mass utilization efficiency for the given channel.

By re-deriving the phenomenological efficiency for multiple channels, the divergence efficiency becomes

$$\eta_d = \left[\sum_i \frac{I_{d,i}}{I_d} \cos \theta_i \right]^2, \tag{18}$$

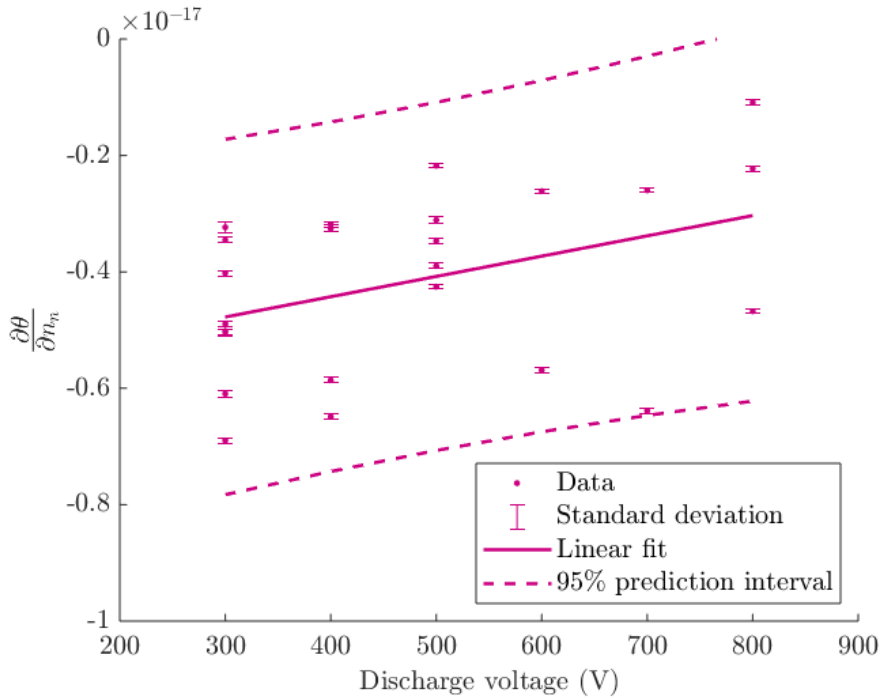

Fig. 2 Measured data and linear fit for change in divergence angle with neutral density as a function of discharge voltage.

where the contribution from divergence angle of each channel is weighted by the current fraction to that channel. We can isolate the increase in efficiency from decreased divergence by comparing this new divergence efficiency term η_d to the efficiency we would see for a single channel η_{d0}:

$$\eta_{d,NHT} = \frac{\eta_d}{\eta_{d0}} = \frac{\left[\sum_i \frac{I_{d,i}}{I_d}\cos\theta_i\right]^2}{\left(\cos\theta_{0,i}\right)^2}. \tag{19}$$

We have now identified our two modified efficiency terms for a nested Hall thruster: efficiency increase due to neutral ingestion from adjacent channels $\eta_{m,NHT}$, and efficiency increase due to decrease in divergence angle $\eta_{d,NHT}$. The final form of anode efficiency can be written as follows, with NHT effects bolded:

$$\eta_a = \eta_{m0}\,\eta_{m,fac}\,\boldsymbol{\eta_{m,NHT}}\,\eta_b\,\eta_v\,\eta_{d0}\,\boldsymbol{\eta_{d,NHT}}, \tag{20}$$

where NHT effects can be grouped as

$$\eta_{NHT} = \eta_{m,NHT}\,\eta_{d,NHT}. \tag{21}$$

Armed with this formulation, we validate our models for correction to mass utilization and divergence by comparing it to experimental data from both the X2 and the X3.[14,15] By comparing theoretical efficiency values to efficiencies measured from X2 and X3 data, we can observe the potential applicability of this expression to other NHTs.

III. Cross-channel Neutral Flow Model

We determine an expression for the geometry factor by modeling the transport of neutrals from adjacent channels j to a given channel i. Figure 3 shows the cross-section of an NHT with two channels and the flow of neutrals from the outer channel to the inner channel. Conical expansion was assumed to be the mechanism by which neutrals travel away from the exit plane of a channel. This model assumes a free molecular flow at the exit plane of the thruster, the usual flow regime for neutrals at the end of the discharge channel in a Hall thruster.[33] This assumption allows us to neglect collisions between particles in the expansion region.

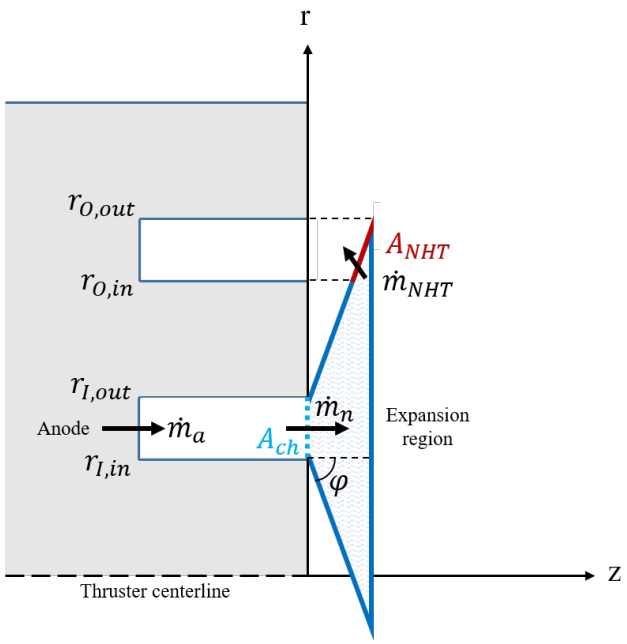

Fig. 3 Section cut showing model of conical expansion of neutrals from outer to inner channel on a two-channel NHT.

The isotropic expansion region A_{exp} is modelled as a trapezoid with angle φ in the r-z plane with one parallel side as the discharge channel from which neutrals are ejected. A constant mass flux is assumed through this expansion area based on the flow regime. When the edge of the cone reaches the line-of-sight of the channel under analysis, the intersecting area is defined as $A_{NHT,j}$. This area is an angled line in the r-z plane, and forms a conical frustrum when rotated for a full revolution about the z-axis. The neutrals travelling through this section are considered to be additional mass flow available for ionization from the adjacent channel. This area was chosen based on previous studies indicating that ionization still occurs outside the exit plane in Hall thrusters.[34,35] However, this region cannot extend infinitely far from the thruster exit plane. Thus, an ionization threshold distance z_{NHT} is defined as the limit of the region that can be ionized by a given channel, shown in Fig. 4. This value is defined as the edge of the FWHM of the magnetic field profile along centerline of a given channel that extends out of the channel.

There are three cases for the location of the ionization threshold as seen in Fig. 4:

1) $z_{NHT} < h_1$: No neutrals are able to cross channels.
2) $h_1 < z_{NHT} < h_2$: Some neutrals are able to cross channels.
3) $h_2 < z_{NHT}$: All allowable neutrals for a given geometry are able to cross channels.

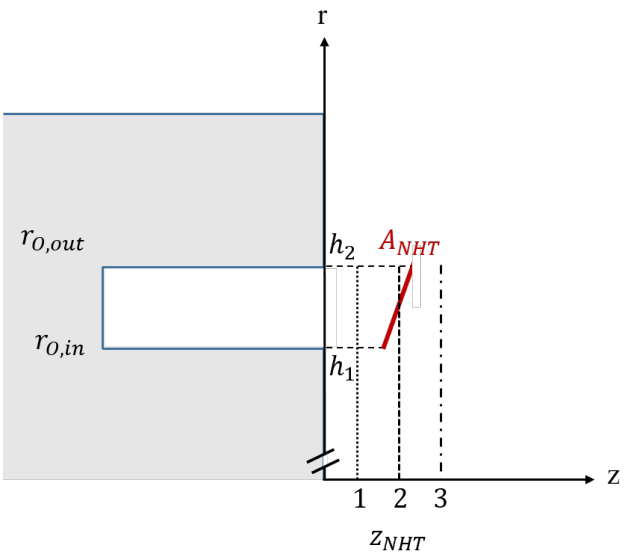

Fig. 4 Close-up section cut of outer channel receiving neutrals and ionization threshold.

For a given set of channels, the thruster geometry defines an upper limit to the size of A_{NHT} and therefore of the amount of neutrals that can travel from one channel to another. The portion of that area that is within an ionizable distance to the thruster is determined by z_{NHT}.

The neutral mass flow across the adjacent channel area, $A_{ch,j}$ (shown in Fig. 3 as a dotted line), is dependent on the mass flow into the anode and the mass utilization efficiency for that channel in single-channel operation. We define the neutral mass flow rate across $A_{ch,j}$ as following:

$$\dot{m}_{n,j} = \dot{m}_{a,j}\left(1 - \eta_{m,j}\right). \tag{22}$$

A constant mass flux exists across the expansion region following our assumption of free molecular flow, yielding the following expression:

$$\Phi = \frac{\dot{m}_{n,j}}{A_{ch,j}} = \frac{\dot{m}_{NHT,ij}}{A_{NHT,ij}}. \tag{23}$$

The channel area is defined as

$$A_{ch,j} = \pi\left(r_{j,out}^2 - r_{j,in}^2\right). \tag{24}$$

The revolved conical geometry is defined by heights h_1 and h_2 as well as channel geometry, as seen in Fig. 4:

$$A_{NHT,ij} = \pi\left(r_{i,in} + r_{i,out}\right)\sqrt{\left(r_{i,out} - r_{i,in}\right)^2 + \left(h_{i,2} - h_{i,1}\right)^2}. \tag{25}$$

For case 1 where the ionization threshold falls below h_1, this area term goes to zero; for case 2 where the ionization region falls between h_1 and h_2, the h_2 term used in Eq. 25 should be set to the threshold value z_{NHT}.

Combining Eq. 22, 23, 24, and 25 gives the following expression for neutral mass ingestion from

adjacent channels j into given channel i:

$$\dot{m}_{NHT,i} = \sum_j \dot{m}_{a,j}\left(1-\eta_{m,j}\right)\frac{A_{NHT,ij}}{A_{ch,j}}. \tag{26}$$

By comparing Eq. 26 to Eq. 14, we can define the geometry factor for the effect of cross-channel neutral ingestion from channel j by channel i:

$$\gamma_{ij} = \left(1-\eta_{m,j}\right)\frac{A_{NHT,ij}}{A_{ch,j}}. \tag{27}$$

It should be noted that this is a model for the influx of neutrals to adjacent channels and therefore assumes nothing of the ionization rate; the neutrals are subject to the same probability of ionization as the rest of the propellant flowing into the channel in the form of the mass utilization efficiency. It is clear from Eq. 26 that for a channel with perfect mass utilization efficiency, the cross-channel neutral flow rate goes to zero as there are no neutrals left to travel out of the channel. A full analysis of how different parameters affect this model is shown in Section IV.

IV. Results

In this section we aim to address how the model scales with various parameters and how well it predicts multi-channel efficiency boosts based on thruster geometry and single-channel performance. Due to the lack of divergence angle data for the X3, an analysis of only the mass utilization efficiency improvement $\eta_{m,NHT}$ was performed for the parametric investigation and comparison of experimental to theoretical data on the X3. A comparison of the divergence utilization efficiency improvement $\eta_{d,NHT}$ is presented for the X2.

A. Parametric Investigation

Before investigating the effect of thruster geometry $\eta_{m,NHT}$, we first needed to determine a reasonable value of φ for our conical expansion model. We did so by comparing the experimental values for $\eta_{m,NHT}$ to the values predicted by the model for angles from 75 to 90 degrees in 5-degree increments. It was found that an expansion angle of $\varphi = 80°$ yielded the best agreement between theoretical and experimental values. Additionally, the experimental efficiencies fell between the points of no contribution (case 1) and maximum contribution (case 3), capturing the impact of z_{NHT}.

Next, four parameters were varied to determine their significance on the efficiencies calculated by the model for a set of two channels. These tuneable parameters reflect the geometry and operating conditions of the thruster, where I indicates the inner and O the outer channel:

1) The ratio between channel centerlines, $\frac{r_I}{r_O}$.
2) The ratio between channel widths, $\frac{w_I}{w_O}$.
3) The ratio between non-NHT neutral mass flow rates, $\frac{(\dot{m}_a+\dot{m}_{fac})_I}{(\dot{m}_a+\dot{m}_{fac})_O}$.
4) The ionization threshold location, z_{NHT}.

To test each of the parameters individually, we held all three other values constant at a value approximately equal to characteristic values seen on the X2 and X3. The resulting trends are shown in Fig. 5.

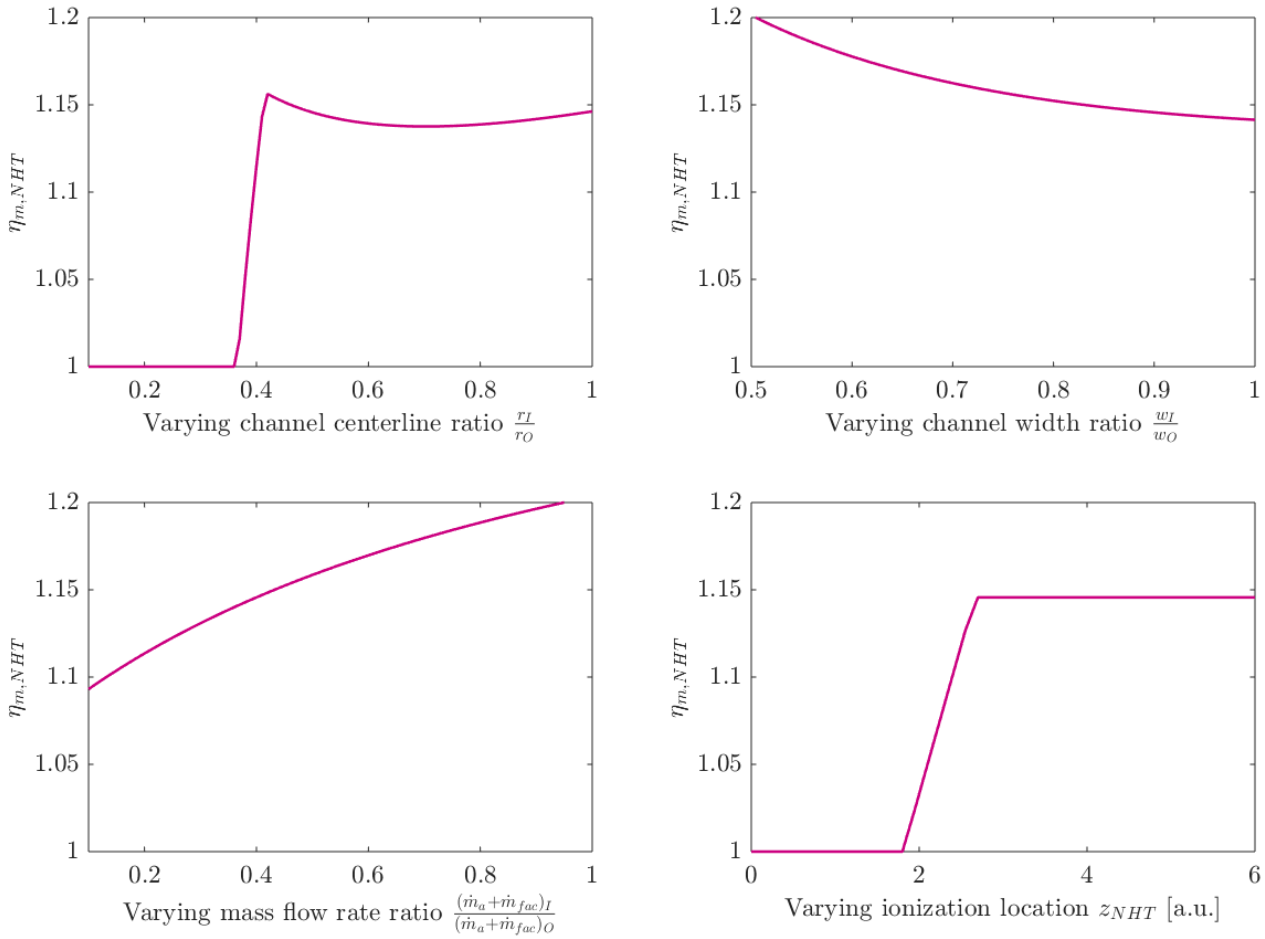

Fig. 5 Change in increased mass utilization efficiency from the variance of different parameters.

The plots for varying channel centerline ratio and varying ionization location have distinct piecewise functions. This behavior is due to the discretized nature of the model itself; as described in Section III, the location of the ionization threshold relative to the region of cross-channel transport can lead to a given channel receiving none, some, or all of the possible cross-channel neutrals. Since there is an instantaneous point where $\eta_{m,NHT}$ starts increasing and an another instant where it stops increasing, the piecewise behavior of these plots makes sense.

From Fig. 5, it would appear that channel centerline ratio (i.e. the distance between channels) and the location of the ionization threshold (i.e. the distance to which the FWHM of the B-field extends out of the thruster) are the two main drivers of the magnitude of efficiency increase from neutral ingestion. However, the actual ranges seen for these values from the X2 and X3 geometries and operating conditions are shown in Table 1.

By viewing only the relevant ranges over which each of these parameters vary in Fig. 5, it becomes apparent that we are in the constant region of the z_{NHT} plot. The distance between channel centerlines, expressed in the form of $\frac{r_I}{r_O}$, emerges as the primary driver of the cross-channel efficiency increase. Once two channels are sufficiently close together, there is a rapid ascent in efficiency augmentation; once those channels are sufficiently far apart, there is no efficiency increase altogether.

Table 1 Ranges of parametric values seen for X2 and X3.

Parameter	$\frac{r_I}{r_O}$	$\frac{w_I}{w_O}$	$\frac{(\dot{m}_a+\dot{m}_{fac})_I}{(\dot{m}_a+\dot{m}_{fac})_O}$	z_{NHT}
Range	0.2 – 0.7	0.2 – 0.7	0.8 – 1	3 – 5 [a.u.]

This dependence matches both with previous evidence[15] and with our physical intuition, as channels that are sufficiently far from each other should not see any significant efficiency increase. However, since the model formulated in this study is so rigid in its discrete nature, more gradual effects at the transitional points could exist that are not captured.

The effect of channel width ratio over the range of seen values is minimal at a change of $\Delta\eta_{m,NHT} = 0.01$ while the impact of mass flow rate ratio is greater at a change of nearly $\Delta\eta_{m,NHT} = 0.07$. While a more balanced flow between channels yields slightly better performance than a smaller ratio, the most influential parameter remains the distance between channels.

B. Comparison to Experimental Data

Theoretical values for $\eta_{m,NHT}$ were calculated based on thruster geometry and operating conditions as well as facility mass flow rates based on Frieman's model[28] using Eqs. 13, 24, 25, and 26. These values were compared to the experimentally measured values for the X2[14] and the X3.[15] The resultant comparisons are shown in Fig. 6.

In Fig. 6, the various terms on the horizontal axis indicate different channel combinations, where I is the inner, M the middle, and O the outer channel. The black dashed line at $\eta_{m,NHT} = 1$ indicates where there is no increase to efficiency at all from cross-channel effects. The lack of error seen for the theoretical value of X3 IO is due to the location of the ionization threshold; because z_{NHT} is sufficiently close to the thruster for this case, accounting for the error in measurements does not change the location or area of A_{NHT} enough to intersect z_{NHT}. Consequently, the model predicts no increase for this condition.

It can be seen that all the modeled efficiencies fall within the uncertainty of the experimental values. However, due to the large uncertainties, it is perhaps more elucidating to investigate trends seen across channel combinations. The model does capture the decrease in efficiency for the X3 IO channel combination, which we expect from our parametric study due to the large distance between these two channels. While the model does make only a preliminary attempt at this by finding no efficiency increase at all, this result does make sense when compared to the other efficiency values. Additionally, the X3 IMO channel combination was the highest among X3 channel combinations for both the theoretical and experimental data. This is also expected due to the contribution of neutrals from multiple adjacent channels for each operational channel. With the exception of the X3 IO condition, all modeled values consistently over-predict experimental values by 3–6%.

We also calculate the total expected efficiency increase from both neutral ingestion and plume divergence for the X2. For the calculation of $\eta_{d,NHT}$, a linear fit for the change in divergence angle due to change in neutral density $\frac{\partial\theta}{\partial n_n}$ based on operating voltage V_d was formulated from an array of facility pressure studies.[30–32] In combination with divergence angle measurements from single-channel oper-

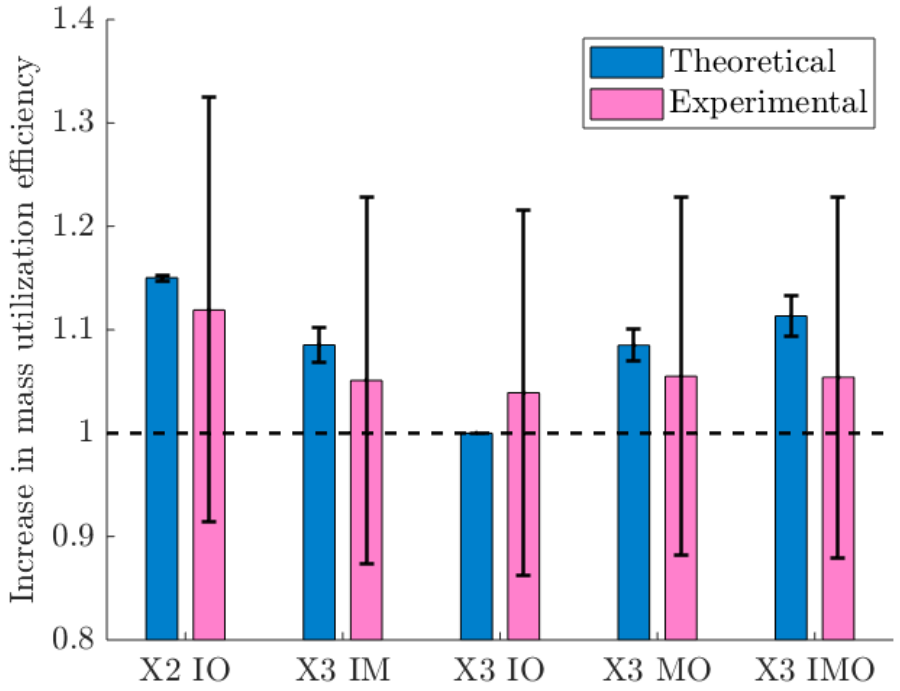

Fig. 6 Theoretical and experimental mass utilization efficiency improvements for different thruster channel combinations.

ation, discharge currents to each channel, and Eqs. 15 and 17, this value allows us to determine the change in divergence angle and therefore improvement in divergence utilization efficiency as defined by Eq. 19. These results are shown in Fig. 7.

As was the case with all mass utilization efficiencies, the different efficiency values for the X2 are all found to agree within uncertainty between the theoretical and experimental values. However, while the mass utilization efficiency over-predicts the change in efficiency, the divergence utilization efficiency under-predicts this improvement. This could be due to error in the linear fit for $\frac{\partial \theta}{\partial n_n}$ as seen in Eq. 16. If this relation with voltage is not linear or if the fit parameters are underestimating the actual impact of facility pressure, the predicted change in divergence could be too small.

V. Discussion

In this section we will discuss the implications of our model and its results, as well as its limitations and ways it could be improved upon in future iterations. The results and trends shown in Fig. 6 and 7 indicate that if equipped with values of thruster geometry and certain measurements from single-channel operation, we are able to predict the increase in efficiency due to cross-channel effects for multi-channel operation within uncertainty. The inputs for these models are the radius, width, current, divergence angle, and mass utilization efficiency for each channel in single-channel operation; the outputs are the increase in mass utilization efficiency and divergence efficiency for the thruster at the same discharge power and mass flow rate per channel. This presents an avenue towards characterizing and predicting the behavior of NHTs without having to perform full-scale tests.

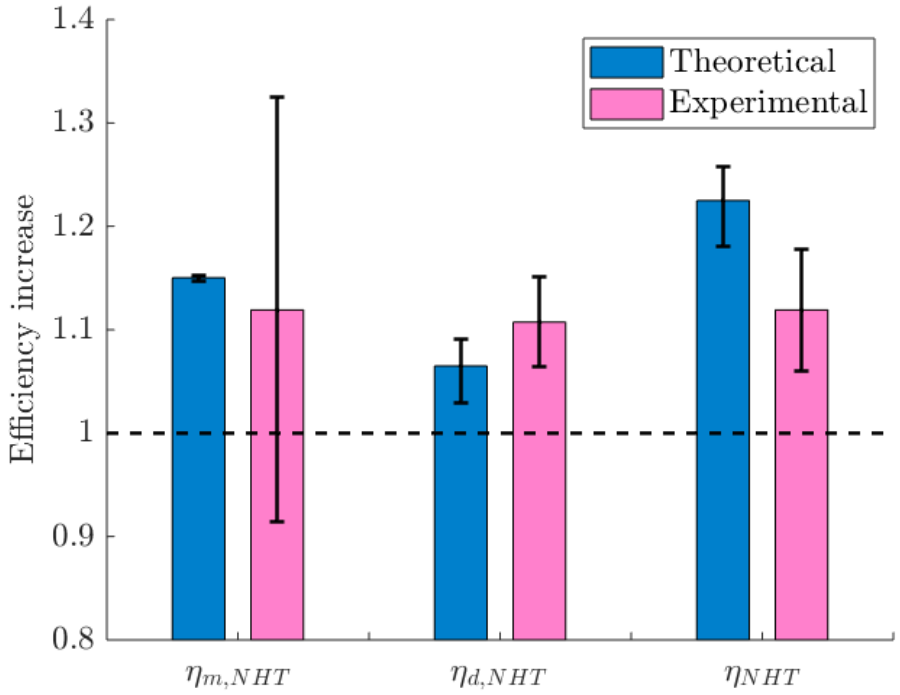

Fig. 7 Theoretical and experimental efficiency improvements for the X2.

One key finding of this study is that to optimize the efficiency boost from cross-channel effects on NHTs, channels should be located fairly close together. However, one feature of the plot of centerline ratios shown in Fig. 6 is that the efficiency only drastically increases from zero up to $\eta_{m,NHT} = 1.16$ at a ratio of $\frac{r_I}{r_O} = 0.42$. After this point, the efficiency actually decreases slightly before increasing slightly again as the channel ratio increases towards 1. This implies that there is a specific threshold of distance between centerlines under which channels on an NHT are able to benefit from the un-ionized neutrals of adjacent channels. Therefore, it is not necessary to place the channels as close as possible, which would be difficult from an engineering perspective due to the scaling laws of optimal Hall thruster channels and the physical size of the magnetic circuit.

The efficiency model breaks down when there are significant portion of multiply-charged ions and when there are significant differences in the current and/or voltage utilization efficiencies between channels. These were key assumptions we made in order to formulate our efficiency model for cross-channel effects. However, there is evidence that the charge utilization efficiency can be significant, especially at higher powers;[15,18] this could mean that the X3 predicted efficiencies are less accurate than the X2 values due to the higher operating powers of the X3. Additionally, the variance of current and voltage utilization efficiencies with mass flow rate and current[18] may mean that these values do not actually hold constant between channels. This model would need to be re-derived and refined to include the effect of multiply-charged ions and the effect of different current and voltage utilization efficiencies.

As for the model of neutral expansion, it would be useful to formulate a higher-fidelity model. As previously mentioned, the current model of conical expansion has discrete regions of no neutral mass flow and maximum neutral mass flow, resulting in instantaneous points where the benefits of cross-

channel flow can or cannot be accounted for. A jet-like expansion from the channel instead of a constant mass flux could lend some precision to this model. Additionally, this model does not take into account neutrals from the cathode. While the cathode flow fraction is usually fairly low on a Hall thruster and therefore supplies minimal neutrals to the channel flows, the X3 in particular had very high flow rates and required external neutral injectors around the cathode to meet satisfactory operation. These additional neutrals could further enhance the efficiencies predicted by the model.

Useful future work includes a fuller set of experimental data, which would be eminently helpful towards determining the accuracy of this model. Specifically, divergence angle measurements could allow us to perform a parameter-based analysis for $\eta_{d,NHT}$ similar to the one performed for $\eta_{m,NHT}$. We can speculate on what this analysis would look like, since the divergence efficiency improvement also relies on the cross-channel flow rate, $\dot{m}_{NHT}$, so it is expected that this efficiency would also scale to some degree with the same parameters. However, having actual experimental measurements and being able to optimize them for less error and the purposes of this model would allow us to verify the validity of this cross-channel efficiency model.

VI. Conclusions

In this work we have re-derived a phenomenological model for Hall thruster efficiency, taking multiple channels into account. This allowed us to more accurately determine which mechanisms contribute the most to efficiency losses on NHTs and if these mechanisms differ from those of their single-channel counterparts. We constructed a model for neutral ingestion between channels of un-ionized propellant based on an conical expansion model with constant mass flux, as well as a model for plume divergence changes due to neutral density increases based on previous studies and a first-order Taylor expansion. We investigated trends in the model by varying different parameters individually. After inputting empirical data into our models, the results were applied to the newly-derived forms for efficiency increases in mass utilization and in plume divergence.

The most influential parameter for cross-channel mass utilization efficiency increases in multi-channel operation was found to be the distance between channels. As the distance increases, the efficiency enhancement can drastically decrease from 15% to none. The ratio between neutral mass flow rate (i.e. including both the anode and facility flows) to the inner and outer channels also had an impact on this efficiency augmentation, with more balanced ratios yielding up to a 7% improvement in efficiency.

Empirical data from the X2 and X3 were compared to the theoretical values from the model. The modeled mass utilization efficiencies matched both the magnitudes and trends seen for different channel combinations on both thrusters to within uncertainty. With the model, we found that the X3 IO condition received no efficiency enhancement from neutral ingestion, attributed to the great distance between the two channels. The plume divergence efficiency was also calculated for the X2; both this value and the total efficiency increase from cross-channel effects were found to match experimentally measured values to within uncertainty. These findings indicate that our model is capable of predicting multi-channel performance based on measurements of single-channel performance and thruster geometry. By showing that we can understand and predict these effects, our results represent an initial step in developing a detailed, semi-empirical approach to accurately predicting the performance of NHTs and advancing the operation of this enabling technology.

VII. Acknowledgements

This work was supported by the Graduate Research Fellowship Program from the National Science Foundation and NASA Space Technology Research Fellowship grant NNX15AQ43H. The authors would also like to thank the members of PEPL for insightful conversation.

References

[1] Myers, R. and Carpenter, C., "High Power Solar Electric Propulsion for Human Space Exploration Architectures," *32nd International Electric Propulsion Conference*, Wiesbaden, Germany, 2011, pp. 2011–261.

[2] Myers, R., Joyner, C., Cassady, R., Overton, S., Kokan, T., Horton, H., and Hoskins, W., "Affordable Exploration Architectures Using the Space Launch System and High Power Solar Electric Propulsion," *34th International Electric Propulsion Conference*, Kobe, Japan, 2015, pp. 2015–492.

[3] Strange, N., Merrill, R., Landau, D., Drake, B., Brophy, J., and Hofer, R., "Human Missions to Phobos and Deimos Using Combined Chemical and Solar Electric Propulsion," *47th AIAA Joint Propulsion Conference*, American Institute of Aeronautics and Astronautics, AIAA-2011-5663, San Diego, CA, 2011.

[4] Brophy, J., Gershman, R., Strange, N., Landau, D., Merrill, R., and Kerslake, T., "300-kW Solar Electric Propulsion System Configuration for Human Exploration of Near-Earth Asteroids," *47th AIAA Joint Propulsion Conference*, American Institute of Aeronautics and Astronautics, AIAA-2011-5514, San Diego, CA, 2011.

[5] Choueiri, E. Y., "Fundamental difference between the two Hall thruster variants," *Physics of Plasmas*, Vol. 8, No. 11, nov 2001, pp. 5025–5033.

[6] Hall, S. J., Jorns, B., Gallimore, A., and Hofer, R. R., "Expanded Thruster Mass Model Incorporating Nested Hall Thrusters," *53rd AIAA/SAE/ASEE Joint Propulsion Conference*, American Institute of Aeronautics and Astronautics (AIAA), Atlanta, GA, jul 2017, pp. 2017–4729.

[7] Jacobson, D., John, J., Kamhawi, H., Manzella, D., and Peterson, P., "An Overview of Hall Thruster Development at NASA's John H. Glenn Research Center," *Joint Propulsion Conference, AIAA-2005-4242*, American Institute of Aeronautics and Astronautics, Tucson, AZ, 2005.

[8] Liang, R., *The Combination of Two Concentric Discharge Channels into a Nested Hall-Effect Thruster*, Ph.D. thesis, University of Michigan, Ann Arbor, MI, 2013.

[9] Jorns, B., Gallimore, A., Hall, S., Peterson, P., Gilland, J., Goebel, D., Hofer, R., and Mikellides, I., "Update on the Nested Hall Thruster Subsystem for the NextSTEP XR-100 Program," *Joint Propulsion Conference, AIAA-2018-4418*, American Institute of Aeronautics and Astronautics, Cincinnati, OH, 2018.

[10] Florenz, R., Hall, S., Gallmiore, A., Kamhawi, H., Griffiths, C., Brown, D., Hofer, R., and Polk, J., "First Firing of a 100-kW Nested-channel Hall Thruster," *33rd International Electric Propulsion Conference*, The George Washington University, USA, 2013, pp. 2013–394.

[11] Hall, S. J., Jorns, B. A., Gallimore, A. D., Kamhawi, H., Haag, T. W., Mackey, J. A., Gilland, J. H., Peterson, P. Y., and Baird, M. J., "High-Power Performance of a 100-kW Class Nested Hall Thruster," *35th International Electric Propulsion Conference*, Atlanta, GA, 2017, pp. 2017–228.

[12] Shark, S. W., Hall, S. J., Jorns, B. A., Hofer, R. R., and Goebel, D. M., "High Power Demonstration of a 100 kW Nested Hall Thruster System," *AIAA Propulsion and Energy 2019 Forum*, Indianapolis, IN, 2019.

[13] Mikellides, I., Katz, I., and Hofer, R., "Design of a Laboratory Hall Thruster with Magnetically Shielded Channel Walls, Phase I: Numerical Simulations," *Joint Propulsion Conference, AIAA-2011-5809*, American Institute of Aeronautics and Astronautics, San Diego, CA, 2011.

[14] Cusson, S., Georgin, M., Dragnea, H., Dale, E., Dhaliwal, V., Boyd, I., and Gallimore, A., "On channel interactions in nested Hall thrusters," *Journal of Applied Physics*, Vol. 123, 2018, pp. 133303.

[15] Hall, S. J., *Characterization of a 100-kW Class Nested-Channel Hall Thruster*, Ph.D. thesis, University of Michigan, Ann Arbor, MI, 2018.

[16] Walker, M. L. and Gallimore, A. D., "Hall thruster cluster operation with a shared cathode," *Journal of Propulsion and Power*, Vol. 23, No. 3, may 2007, pp. 528–536.

[17] "Performance characteristics of a cluster of 5-kW laboratory hall thrusters," *Journal of Propulsion and Power*, Vol. 23, No. 1, jan 2007, pp. 35–43.

[18] Hofer, R. R. and Gallimore, A. D., "Efficiency Analysis of a High-Specific Impulse Hall Thruster," *40th*

Joint Propulsion Conference, AIAA-2004-3602, American Institute of Aeronautics and Astronautics, Ft. Lauderdale, FL, 2004.

[19] Hofer, R. R., Katz, I., Mikellides, I. G., Goebel, D. M., Jameson, K. K., Sullivan, R. M., , and Johnson, L. K., "Efficacy of Electron Mobility Models in Hybrid-PIC Hall Thruster Simulations," *44th Joint Propulsion Conference, AIAA-2008-4924*, American Institute of Aeronautics and Astronautics, Hartford, CT, 2008.

[20] Hofer, R. R., *Development and Characterization of High-Efficiency, High-Specific Impulse Xenon Hall Thrusters*, Ph.D. thesis, University of Michigan, 2004.

[21] Goebel, D. M. and Katz, I., *Fundamentals of Electric Propulsion: Ion and Hall Thrusters*, Jet Propulsion Laboratory, California Institute of Technology, Pasadena, CA, 2008.

[22] Brown, D. L., Larson, C. W., Beal, B. E., and Gallimore, A. D., "Methodology and Historical Perspective of a Hall Thruster Efficiency Analysis," *Journal of Propulsion and Power*, Vol. 25, No. 6, nov 2009, pp. 1163–1177.

[23] Randolph, T., Kim, V., Kaufman, H., Kozubsky, K., Zhurin, V., and Day, M., "Facility Effects on Stationary Plasma Thruster Testing," *23rd International Electric Propulsion Conference*, Seattle, WA, 1993.

[24] Byers, D., Vegas, L., and Dankanich, J. W., "A Review of Facility Effects on Hall Effect Thrusters," *31st International Electric Propulsion Conference*, Ann Arbor, MI, 2009.

[25] Hofer, R. R., Peterson, P. Y., and Gallimore, A. D., "Characterizing Vacuum Facility Backpressure Effects on the Performance of a Hall Thruster," *27th International Electric Propulsion Conference*, Pasadena, CA, 2001, pp. 2001–045.

[26] Nakles, M. R. and Hargus, W. A., "Background Pressure Effects on Ion Velocity Distribution Within a Medium-Power Hall Thruster," *Journal of Propulsion and Power*, Vol. 27, 2012, pp. 737–743.

[27] Reid, B. M. and Gallimore, A. D., "Review of Hall Thruster Neutral Flow Dynamics," *30th International Electric Propulsion Conference*, Florence, Italy, 2007, pp. 2007–038.

[28] Frieman, J. D., Liu, T. M., and Walker, M. L. R., "Background Flow Model of Hall Thruster Neutral Ingestion," *Journal of Propulsion and Power*, Vol. 33, 2017, pp. 1087–1101.

[29] Cusson, S. E., Dale, E. T., and Gallimore, A., "Investigation of Channel Interactions in a Nested Hall Thruster Part II: Probes and Performance," *52nd AIAA/SAE/ASEE Joint Propulsion Conference*, American Institute of Aeronautics and Astronautics (AIAA), Salt Lake City, UT, 2016.

[30] Walker, M., Hofer, R., and Gallimore, A., "The Effects of Nude Faraday Probe Design and Vacuum Facility Backpressure on the Measured Ion Current Density Profile of Hall Thruster Plumes," *38th AIAA/ASME/SAE/ASEE Joint Propulsion Conference & Exhibit*, American Institute of Aeronautics and Astronautics (AIAA), Indianapolis, IN, 2002.

[31] Huang, W., Kamhawi, H., and Haag, T., "Facility Effect Characterization Test of NASA's HERMeS Hall Thruster," *52nd AIAA/SAE/ASEE Joint Propulsion Conference*, American Institute of Aeronautics and Astronautics (AIAA), Salt Lake City, UT, 2016.

[32] Huang, W., Kamhawi, H., Lobbia, R. B., and Brown, D. L., "Effect of Background Pressure on the Plasma Oscillation Characteristics of the HiVHAc Hall Thruster," *33rd International Electric Propulsion Conference*, American Institute of Aeronautics and Astronautics (AIAA), Washington, D.C., 2013.

[33] Huang, W., Gallimore, A. D., and Hofer, R. R., "Neutral Flow Evolution in a Six-Kilowatt Hall Thruster," *Journal of Propulsion and Power*, Vol. 27, No. 3, apr 2011, pp. 553–563.

[34] King, L. B. and Gallimore, A. D., "Ion-Energy Diagnostics in an SPT-100 Plume from Thrust Axis to Backflow," *Journal of Propulsion and Power*, Vol. 20, No. 2, 2004, pp. 228–242.

[35] Mikellides, I., Katz, I., Mandell, M., and Snyder, J., "A 1-D model of the Hall-effect thruster with an exhaust region," *37th AIAA/ASME/SAE/ASEE Joint Propulsion Conference*, American Institute of Aeronautics and Astronautics (AIAA), Salt Lake City, UT, 2011.